Comparative Biochemistry and Physiology, Part A 191 (2016) 202–208

Contents lists available at ScienceDirect

Comparative Biochemistry and Physiology, Part A

journal homepage: www.elsevier.com/locate/cbpa

Circulatory changes associated with the closure of the ductus arteriosus in hatching emu (*Dromaius novaehollandiae*)

Lauren Shell [a], Warren Burggren [a], David Muirhead [b], Thomas C. Nelson [c,1], Edward M. Dzialowski [a,*]

[a] Developmental Integrative Biology Research Group, Department of Biological Sciences, 1155 Union Circle #305220, University of North Texas, Denton, TX 76203, United States
[b] City of Hope, 1500 East Duarte Road, Duarte, CA 91010, United States
[c] Department of Biological Sciences, Kalamazoo College, Kalamazoo, MI 49008, United States

ARTICLE INFO

Article history:
Received 2 September 2015
Received in revised form 30 October 2015
Accepted 3 November 2015
Available online 5 November 2015

Keywords:
Ductus arteriosus
Hatching
Blood shunt
Vascular remodeling
Apoptosis
Vasoconstriction

ABSTRACT

In developing avian embryos, the right and left ductus arteriosi (DA) allow for a shunt of systemic venous return away from the lungs to the body and chorioallantoic membrane (CAM). Unlike in mammals where the transition from placental respiration to lung respiration is instantaneous, in birds the transition from embryonic CAM respiration to lung respiration can take over 24 h. To understand the physiological consequences of this long transition we examined circulatory changes and DA morphological changes during hatching in the emu (*Dromaius novaehollandiae*), a primitive ratite bird. By tracking microspheres injected into a CAM vein, we observed no change in DA blood flow between the pre-pipped to internally pipped stages. Two hours after external pipping, however, a significant decrease in DA blood flow occurred, evident from a decreased systemic blood flow and subsequent increased lung blood flow. Upon hatching, the right-to-left shunt disappeared. These physiological changes in DA blood flow correspond with a large decrease in DA lumen diameter from the pre-pipped stages to Day 1 hatchlings. Upon hatching, the right-to-left shunt disappeared and at the same time apoptosis of smooth muscle cells began remodeling the DA for permanent closure. After the initial smooth muscle contraction, the lumen disappeared as intimal cushioning formed, the internal elastic lamina degenerated, and numerous cells underwent regulated apoptosis. The DA closed rapidly between the initiation of external pipping and hatching, resulting in circulatory patterns similar to the adult. This response is most likely produced by increased DA constriction in response to increased arterial oxygen levels and the initiation of vessel remodeling.

1. Introduction

In developing mammals and birds, embryonic gas exchange occurs by means of the placenta or chorioallantoic membrane (CAM), respectively. Blood bypasses the lungs via an embryonic vascular shunt known as the ductus arteriosus (DA). The DA is derived from the sixth aortic arch and shunts blood away from the pulmonary artery and into the systemic pathway (Slomp et al., 1992; Bergwerff et al., 1999; Dzialowski et al., 2011; Levin et al., 2005; Belanger et al., 2008; Greyner and Dzialowski, 2008). In birds such as the chicken, the DA consists of two discrete sections. The proximal section lies close to the pulmonary artery and is composed mostly of smooth muscle cells. The distal section connects the vessel directly to the aorta and has more elastin and less smooth muscle than the proximal portion of the DA (Belanger et al., 2008; Greyner and Dzialowski, 2008). In the chicken embryo, 16% of the cardiac output from the right ventricle flows to the lungs, likely to provide nourishment for pulmonary development, while the rest passes through the ductus (Rahn et al., 1985).

The embryo uses the DA throughout its development in utero/in ovo and it must close with birth or hatching. As birth/hatching occurs, the embryonic gas exchanger is superseded by pulmonary respiration, and blood must flow through the lungs as the animal begins to breathe atmospheric air. This transition period is accomplished by the constriction of the DA and subsequent remodeling of the vessel walls (Rabinovitch, 1996; Belanger et al., 2008; Yokoyama et al., 2010; Yokoyama, 2015). The developmental period over which the ductus closes varies interspecifically. For mammals, DA closure occurs over several minutes to a few hours, since the switch from placenta to lungs is immediate. In birds, however, this process occurs over a longer paranatal period of several hours or even days as the embryo transitions from the embryonic in ovo stage to the hatchling ex ovo stage of life (Visschedijk, 1968; Rahn et al., 1985). The morphological and physiological changes that occur over this prolonged period of closure in birds are relatively unknown.

Ductus closure generally occurs in two stages: initial functional closure by smooth muscle constriction of the vessel, followed by morphological remodeling of the ductus arteriosus. During the first stage of DA

* Corresponding author. Tel.: +1 940 565 3631; fax: +1 940 565 3821.
E-mail address: edzial@unt.edu (E.M. Dzialowski).
[1] Current Address: Institute of Ecology and Evolution, 335 Pacific Hall, 5289 University of Oregon, Eugene, OR 97403, United States.

http://dx.doi.org/10.1016/j.cbpa.2015.11.006
1095-6433/

closure, smooth muscles contract in response to an increase in arterial PO_2 (Tristani-Firouzi et al., 1996; Thébaud et al., 2004; Reese et al., 2006; Greyner and Dzialowski, 2008; Yokoyama et al., 2010; Coceani and Baragatti, 2012). The DA from both chicken and emu embryos are sensitive to the increase in blood PO_2 that occurs during pipping, hatching, and the associated switch to pulmonary respiration. This increased PO_2 initiates the contraction that takes place in the DA prior to actual morphological remodeling (Tristani-Firouzi et al., 1996; Imamura et al., 2000; Thébaud et al., 2004; Greyner and Dzialowski, 2008; van der Sterren et al., 2014). In the chicken, proximal DA closure begins with smooth muscle contraction during the last stage of hatching, external pipping (Belanger et al., 2008). This constriction has been shown to be redox sensitive and involved the Rho kinase pathway, as well as influx of Ca^{2+} through L-type calcium channels (Keck et al., 2005; Weir et al., 2008; Greyner and Dzialowski, 2008; Cogolludo et al, 2009; Hong et al., 2013).

The morphological changes that remodel the DA after the initial constriction have been studied mainly in mice, rabbits, and monkeys (Tada and Kishimoto, 1990; Giuriato et al., 1993; Rabinovitch, 1996; Clyman et al., 1999; Imamura et al., 2000; Yokoyama et al., 2010; Coceani and Baragatti, 2012; Yokoyama, 2015), with one study in the birds (Belanger et al., 2008). The proximal DA is the first vascular area to begin anatomical remodeling in the chicken, and does so starting on day 20 of incubation when the embryo is externally pipped (Belanger et al., 2008). Over the next 12 to 24 h, fragmentation of the internal elastic lamina occurs and smooth muscle cells migrate into the tunica intima of the vessel resulting in occlusion of the lumen (Belanger et al., 2008). A decrease in the overall number of smooth muscle cells in the DA occurs in the days following mammalian birth (Tennenbaum et al., 1996). Apoptosis also occurs in the mammalian DA, but its presence and timing in the avian DA are unknown. Lamb, sheep, baboon, and human DA have all exhibited marked levels of Terminal deoxynucleotidyl transferase dUTP nick end labeling (TUNEL) positive cells after birth (Clyman et al., 1999; Goldbarg et al., 2003; Levin et al., 2005, 2006; Kim et al., 2009). When closure occurs, the majority of smooth muscle cells in the lamb DA undergo cell death in the first 24 h after birth (Levin et al., 2005). Immature DA that remain patent, on the other hand, do not display a marked level of TUNEL-positive cells (Levin et al., 2005). Baboon DA show the presence of cell death in the most hypoxic areas of the vessel (Clyman et al., 1999) and other studies confirm that hypoxia, along with ATP depletion and hypoglycemia, contribute to the incidence and amount of TUNEL-positive cells in the mammalian DA (Goldbarg et al., 2003; Levin et al., 2005, 2006).

Hatching in the emu (*Dromaius novaehollandiae*) begins after approximately 49 days of incubation (E49), when the bird breaks through the air cell during internal pipping (IP) and begins to respire with its lungs. External pipping (EP) and hatching follow on day 50 when the bird breaks the eggshell with its beak and breathes normoxic air for the first time. The overall process of the onset of pulmonary respiration is prolonged in birds (hours to days; Visschedijk, 1968; Rahn et al., 1985) compared to mammals (a few minutes). Moreover, the circulatory and morphological changes at the DA are unknown in birds beyond the chicken which, although commonly investigated, is not representative of the great diversity among birds. Emu belong to Palaeognathae, among the most primitive clades of birds (Prum et al., 2015) and when compared with other birds and mammals can provide an understanding of potentially conserved developmental morphological and physiological phenotypes in vertebrate lineages. Thus, the main objective of this study was to examine the DA morphological changes, including apoptosis, and associated blood flow patterns occurring in the hatching emu. We hypothesized that the greatest changes in blood flow and DA morphology would occur during the externally pipped stage of the hatching process. To test this hypothesis, we measured changes in blood flow patterns during hatching and the associated morphological changes in the ductus arteriosus of the emu.

2. Methods

2.1. Eggs and incubation

Emu eggs were obtained from the Cross Timbers Emu Ranch in Pilot Point, Texas. Eggs were incubated in a Hatchrite incubator at a temperature of 36.5 °C, relative humidity of 35%, and automatically turned every 4 h. The University of North Texas Animal Care and Use Committee approved all procedures used in this study.

2.2. Blood flow patterns

The distribution of blood flow from the right atrium to the lungs, heart, brain, and CAM was measured in day 49 internally pipped embryos, externally pipped embryos, and day 0 hatchlings, corresponding to 98%, 99%, and 100% of embryonic development. Relative blood flows were measured by determining the distribution of colored microspheres (15 μm diameter in heparinized 0.09% NaCl saline with 0.05% Tween 80, IMT — Stason Laboratory, Irving, CA) in tissues of interest (see Sbong and Dzialowski, 2007), as briefly described below. Embryonic stages were cannulated by removing a small portion of the eggshell and associated membranes to reveal the chorioallantoic membrane. A chronic cannula was inserted into a small chorioallantoic vein using heat-pulled PE 10 tubing. Externally pipped embryos were cannulated during internal pipping and then were artificially externally pipped by breaking a hole into the shell. The animals were allowed to be externally pipped for two hours prior to injection of microspheres.

Hatchlings were cannulated at either the femoral or jugular vein while anesthetized by inhalation of isoflurane and artificially ventilated. Animals were intubated and ventilated using a Harvard ventilator. 50 microliters of colored microspheres (8000 microspheres/μl) in heparinized saline were injected into the CAM vein or jugular vein, where they passed through the right side of the heart and were then distributed to the systemic or pulmonary circuit. Anesthetized embryos and hatchlings were euthanized by decapitation and the heart, brain, CAM, and lungs were removed and weighed. Each tissue was digested overnight in 10–13 ml of 1 M KOH at 65 °C. Sodium deoxycholic reagent was added to the digested tissue to increase the volume to 14 ml. This solution was then mixed by vortex and centrifuged at 1500 *g* for 30 min. The supernatant was aspirated, and the pellet was re-suspended by sonication into 10 ml 5% Triton X-100 solution. The solution was centrifuged at 1500 *g* for 15 min, and the supernatant was aspirated to a level just above the pellet. The remaining volume was determined with a 200 μl pipette. The number of microspheres in each tissue sample was then counted using a hemocytometer. Data are presented as the number of microspheres counted in the CAM, heart, or brain divided by the number of microspheres counted in the lungs. This measure allows estimation of the blood leaving the right atria and flowing to the tissues through the DA and the interatrial foramina, distinct from blood flowing to the lungs through the pulmonary arteries (Dzialowski et al., 2011; Sbong and Dzialowski, 2007). The greater the ratio, the greater the right-to-left shunt of blood away from the lungs and to that tissue.

2.3. Histology

To examine morphological DA closure during hatching, emus were studied on incubation days 45, 50, and 51, and post-hatching days 0, 1, 2, 3, and 4. Birds were euthanized by inhalation of isoflurane and the right DA was removed and fixed in 4% paraformaldehyde at 4 °C for 24 h before being stored in phosphate buffered saline (pH 7.4).

The fixed vessels were dehydrated in graded methanol, infiltrated with paraffin, and then embedded and oriented in paraffin blocks for sectioning. Using a microtome, 5 μm thick sections of DA were sectioned and mounted on microscope slides. Slides were deparaffinized in xylene and rehydrated in graded ethanol. The samples were stained for further morphological analysis with hematoxylin and eosin (H&E).

Serial sections were stained by Van Gieson stain to determine the morphological and histological changes in elastin fibers and the internal elastic lamina of the DA over time. Histomorphometric measurements were made on digital images of the DA sections using ImagePro Plus 5.0 image analysis software (Mediacybernetics) and ImageJ (NIH). The lumen diameter was determined by measuring the lumen circumference and then calculating diameter assuming the DA had a circular configuration (Rouwet et al., 2002; Belanger et al., 2008).

2.4. Apoptosis

Tissues were examined for evidence of apoptosis by staining for terminal deoxynucleotidyl transferase-mediated dUTP nick-end labeling (TUNEL) using the TUNEL Apoptag® Peroxidase In Situ Apoptosis Detection Kit (Millipore). This technique detects fragmented DNA associated with apoptosis resulting in apoptotic nuclei staining brown (Gavrieli et al., 1992). Positive control slides (female rodent mammary gland) were run with each experimental trial as a quality control measure. Images were taken of DA sections and the presence of TUNEL-positive cells was analyzed on day 45, day 49, IP, and EP embryos and on days 0, 1, and 2 post-hatching. For each sample, an apoptosis index was determined by examining the sections at a 40× objective setting on a Nikon E2000 microscope and counting the number of apoptotic nuclei within the field of view. All vessel structures, including the tunica adventitia, were included in the quantitative analysis.

2.5. Statistics

Masses were compared by ANOVA followed by Holm–Sidak post hoc test. Blood flow changes were examined after log transformation with one-way ANOVA. This was followed by Holm–Sidak post hoc test to determine when blood flow differed significantly from embryonic day 49. Lumen diameters were compared during development with a one-way ANOVA followed by Holm–Sidak post hoc test compared against day 45 DA diameter. Lumen diameters and blood flow data are presented as the mean ± standard error (SE). The presence of TUNEL-positive cells was examined using an ANOVA on ranks followed by Dunn's post hoc test. TUNEL-positive cell data is presented as the median and 25th and 75th percentile. Significance was taken at $p < 0.05$. Statistics were run on SigmaPlot 11.

3. Results

3.1. Masses

There were no significant differences in yolk-free body mass between pre-pipped embryos, internally/externally pipped embryos, and hatchlings ($p = 0.770$; Table 1). However, heart mass increased significantly across these developmental landmarks ($p < 0.001$; Table 1). Heart mass increased between pre-pipped and IP embryos and remained elevated in hatchlings. Heart mass as a function of body mass increased from ~0.4% of body mass during EP to 0.6% as a hatchling. Left lung mass also increased during this period ($p = 0.005$), being largest in the IP/EP embryos.

Table 1
Mean yolk-free body mass, heart mass, and left lung mass of emus. Values with different letters are significantly different from each other. Data is presented at mean ± standard deviation.

	Pre-pipped	IP/EP	Hatchling
Yolk-free body mass (g)	253.1 ± 42.8 (11)	232.6 ± 66.0 (3)	250.0 ± 33.7 (7)
Heart mass (g)	1.06 ± 0.26[a] (11)	1.42 ± 0.23[b] (5)	1.55 ± 0.25[b] (10)
Lung mass (g)	0.88 ± 0.23[a] (11)	1.59 ± 0.59[b] (5)	1.15 ± 0.34[a,b] (10)

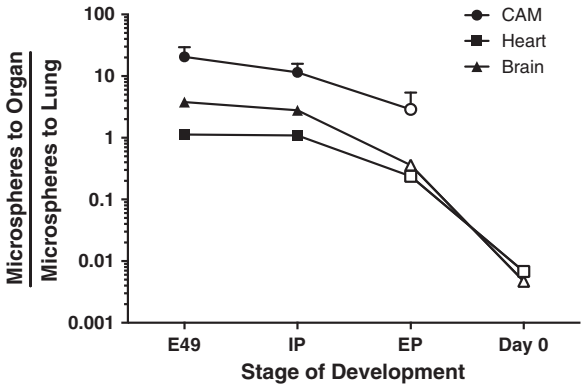

Fig. 1. Changes in blood flow through the ductus arteriosus during hatching in the emu, reported as the ratio of the number of microspheres found in the CAM (circle), heart (square), and brain (triangle) to the number of microspheres found in the lungs as a function of stage of development. A decrease in the ratio indicates an increase in pulmonary flow through the pulmonary artery and a decrease in the right-to-left shunt. E49, embryo day 49 ($n = 10$); IP, internally pipped ($n = 5$); EP, externally pipped ($n = 5$); hatchling ($n = 10$). Data presented as means ± SE. Open symbols represent a significant ($P < 0.05$) decrease compared with the day 49 embryos.

3.2. Right atrial blood flow

There was a significant decrease in the right-to-left shunt of blood (i.e., pulmonary bypass) leaving the right atria and flowing to the CAM ($p = 0.002$), heart ($p < 0.001$), and brain ($p < 0.001$) during hatching (Fig. 1). In day 49 embryos, blood flow from the right atria to the CAM and to the brain was 20 and 4 times greater, respectively, than the blood flow to the lungs. During the transition from E49 to IP there was little change in blood flow distribution from the right atria to the four tissues. Upon EP, however, right-to-left shunting of blood decreased significantly. This was evident from a decrease in blood flow to the CAM, heart, and brain relative to the flow to the lungs during this stage of hatching. After hatching, the right-to-left shunt disappeared, with the great majority of the microspheres ultimately captured in the lung.

3.3. Ductus morphology

Progressive, significant constriction of the DA lumen ($p < 0.001$) occurred during the paranatal hatching period from a mean around 0.5 mm prior to hatching (Fig. 2A). While lumen diameters were not significantly different from each other on days 45, day 49, and IP, upon external pipping, DA lumen diameter decreased significantly when compared with embryonic day 45 DA ($p < 0.001$). This constriction progressed through day 4 post-hatching, at which point the lumen was functionally occluded, with a diameter not significantly different from zero.

Mean DA wall thickness, taking into account the entire vessel including the tunica adventitia, increased in size between E45 and E49 (Fig. 2B). As the vessel constricted and the wall thickness increased, the smooth muscle cells decreased in length and the endothelial cells and neointimal zone increased in thickness.

The DA exhibited significant morphological changes during hatching (Fig. 3). On day 45 of incubation the DA was composed of a well-defined smooth muscle layer surrounded by an elastic layer (Fig. 3A & B). The smooth muscle layer was typically arranged in 8 to 11 layers of smooth muscle cells. The vessel had a large lumen with a well-defined internal elastic lamina and single layer of endothelial cells in the tunica intima. There was little morphological change occurring from E45 to E49. The first distinct morphological change began during IP, with the lumen narrowing compared with E45 and E49 embryos (Fig. 3C & D). An additional change between the embryonic stage and the IP stage was the

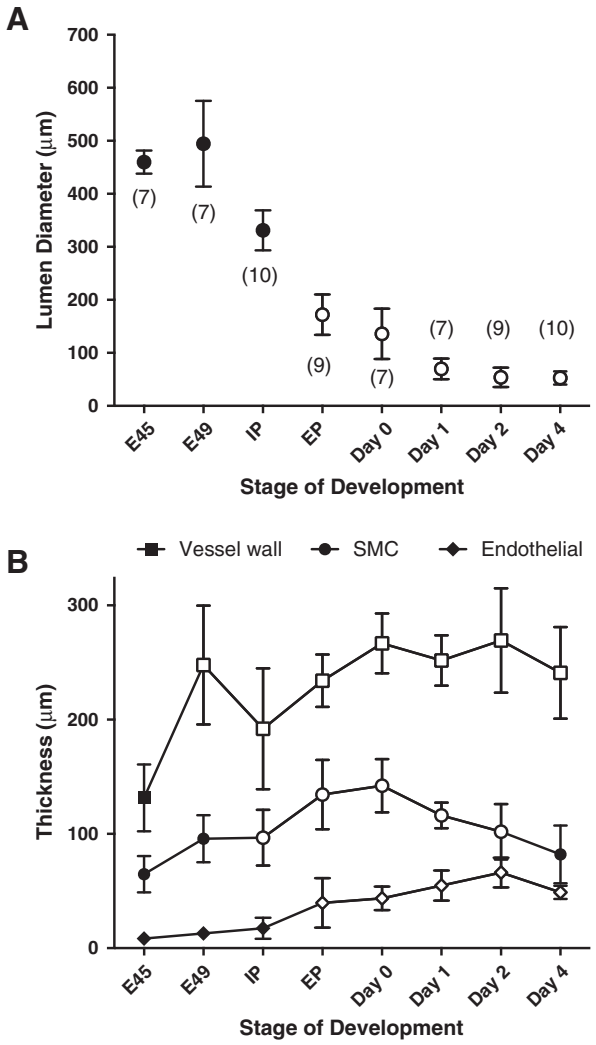

Fig. 2. A) Lumen diameter (μm) and B) vessel thickness (μm) of the fixed right DA as a function of stage of development. Sample sizes are provided in the parentheses. Data presented as means ± SE. Open symbols represent a significant ($P < 0.05$) change compared with the day 45 embryos.

development of intimal cushions at the endothelial layer surrounding the lumen. During EP, the intimal cushions became more pronounced and averaged 2 cells thick (Fig. 2E & F). Additionally, the lumen at EP was greatly reduced from its original size compared with E45 and E49 embryos. Van Gieson staining revealed that there was fragmentation of the internal elastic lamina occurring during the paranatal period. On day 0 (hatchling) the intimal cushions were ~4 cells thick, and the lumen diameter was markedly smaller than the diameter of the EP lumen. Day 1 and day 2 hatchlings showed a functionally closed lumen and a breakdown of the internal elastic lamina (Fig. 2G & H). As the smooth muscle cells contracted, the nuclei revealed a rearrangement of the layer.

3.4. Apoptosis

Significant apoptosis of DA smooth muscle cells occurred upon hatching. TUNEL-positive cells, signaling apoptosis of smooth muscle cells in the DA, first appeared during the IP stage of hatching and increased significantly after hatching ($p < 0.001$; Figs. 4, 5A). On days E45 and E49, none of the DA sections examined contained TUNEL-positive smooth muscle cells (Fig. 5A). The first signs of apoptosis appeared in DA vessels from IP emu (Fig. 4). Of 5 animals examined, one showed TUNEL-positive cells (15 cells). TUNEL-positive cells were observed in all EP DA examined (Fig. 4) with a median number of 15 TUNEL-positive counted per field of view (Fig. 4). There was a small, insignificant increase in the number of TUNEL-positive cells in the DA from day 0 hatchlings (median value of 39 positive cells per field of view). By days 1 and 2, the number of TUNEL-positive cells were significantly greater than E 45 embryos ($P < 0.05$), showing a median of 124 and 147 TUNEL-positive cells in the DA, respectively (Figs. 4, 5B).

4. Discussion

4.1. Hemodynamic changes during hatching

Compared with mammals, the emu (like most birds) has an extended hatching period as it transitions from the in ovo embryonic gas exchanger to ex ovo lung ventilation. Associated with this extended transition is a slow closure of the ductus arteriosus lasting from internal pipping through the first day of posthatch life — as long as 1–2 days. It is unclear how this extended period of hemodynamic transition in the emu or other birds varies from that in mammals. Indeed, this is the first study to document the hemodynamic changes as well as identify signs of remodeling-associated apoptosis in an avian ductus arteriosus. During hatching, the greatest change in flow through the right-to-left shunt provided by the DA occurred during the transition from the externally pipped embryo to the hatchling (Fig. 2). This is in contrast to chickens, where changes in the right-to-left shunt begin upon internal pipping and continue through hatching (Rahn et al., 1985). The present study has used the declining magnitude of the right-to-left shunt as one indicator of closure of the ductus arteriosus in the emu. In mammals such as the neonatal lamb, there is a reversal of blood flow through the DA that occurs immediately after birth as the animal begins to respire with its lungs (Kajino et al., 2002), quickly followed by functional closure of the DA and with that, of course, no further right-to-left shunt via this pathway. Blood flow changes in the emu suggest that there should be minimal reversal of flow and unlike in mammals a right-to-left shut is maintained, albeit at a lower level, once lung ventilation begins during the IP stage.

4.2. Morphological changes during hatching

Prior to hatching, the emu DA has a patent functional lumen. The vessel walls consist of a lining layer of endothelial cells, an internal elastic lamina, a tunica media composed mainly of 2–3 layers of smooth muscle cells, and a tunica adventitia where the vasa vasorum are located. Hatching begins with the IP stage on day 49. At this point the endothelial cells break away from the internal elastic lamina and intimal cushions begin to form. The physiological signal that initiates smooth muscle cell contraction during DA closure is the quickly elevating blood oxygen levels associated with the initiation of lung ventilation (Imamura et al., 2000; Greyner and Dzialowski, 2008). Intimal cushions occur when the endothelial cells lining the lumen of the DA detach from the internal elastic lamina, and smooth muscle cells collect in the neointimal zone, the space between the internal elastic lamina and the endothelium layer (Clyman et al., 1999; Slomp et al., 1992; Belanger et al., 2008). Previous studies have characterized DA intimal cushions in other animals such as humans, chickens, and rabbits (Slomp et al., 1992; Giuriato et al., 1993; Belanger et al., 2008). In the emu beginning at IP, the internal elastic lamina undergoes fragmentation demonstrated by Van Gieson staining, and the intimal cushions increase in size until the lumen is fully blocked by smooth muscle cells on post-hatch day 2.

The increased presence of smooth muscle cells in the neointimal zone has been described in humans due to the migration of modified smooth muscle cells from the tunica media (Slomp et al., 1992) and in the chicken aorta, as the proliferation of smooth muscle cells from the differentiation of endothelial cells (Arciniegas et al., 2000). In the emu, intimal cushions were present at the beginning of the IP stage of hatching following the initial contraction of the DA. These intimal cushions

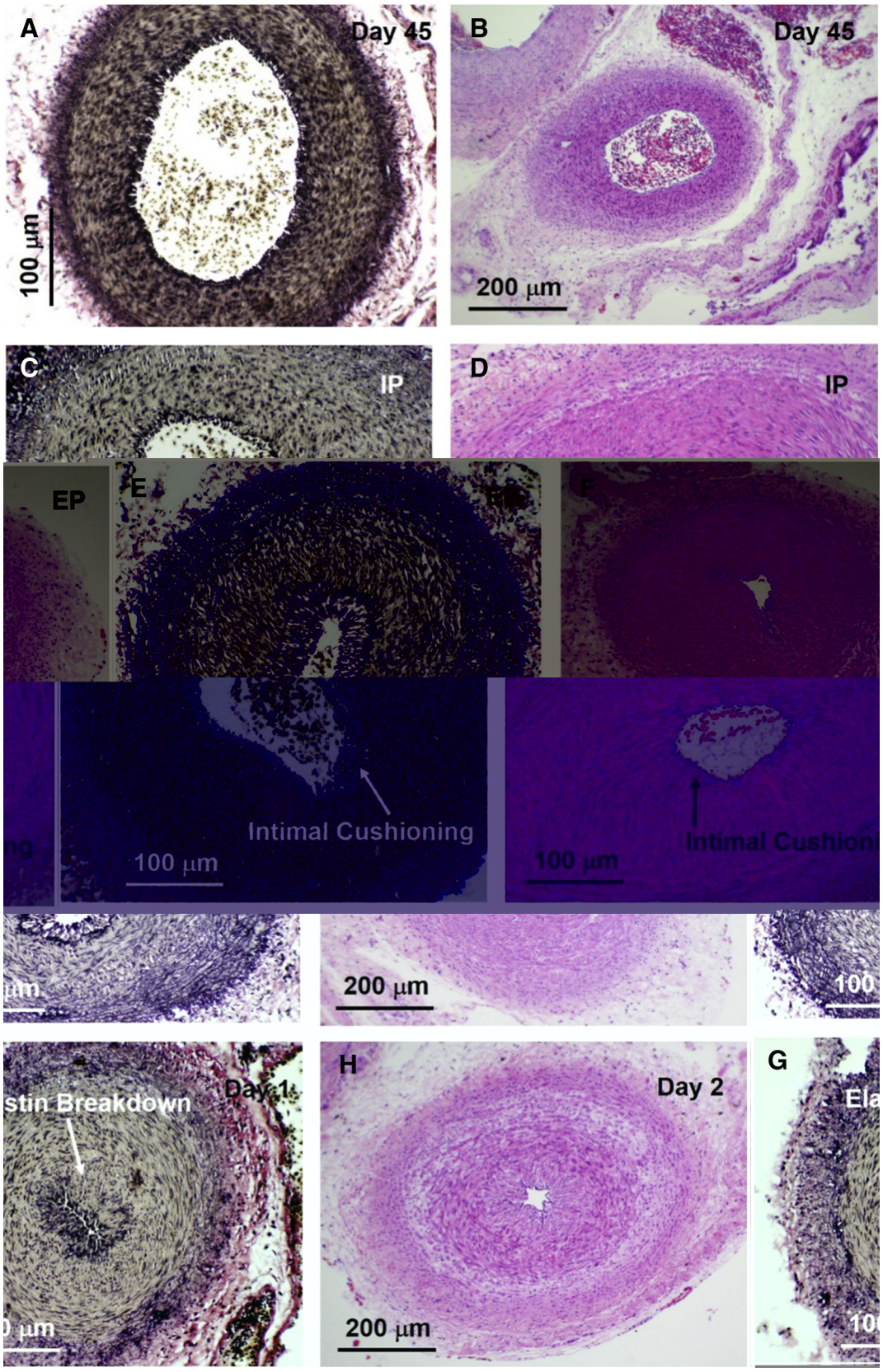

Fig. 3. Histological sections of the left and right proximal DA observed under a compound light microscope. Left proximal vessels (A, C, E, G) were stained using the Van Gieson method to view elastin fibers, while right proximal vessels (B, D, F, H) were stained with hematoxylin and eosin. At day 45 the lumen diameter is large and unobstructed (A, B). Intimal cushions begin to form during IP (C, D). The lumen decreases further in diameter during EP (E, F). At day 0 extensive fragmentation of the internal elastic lamina occurs (G). The lumen is fully closed on day 2 after hatching (H).

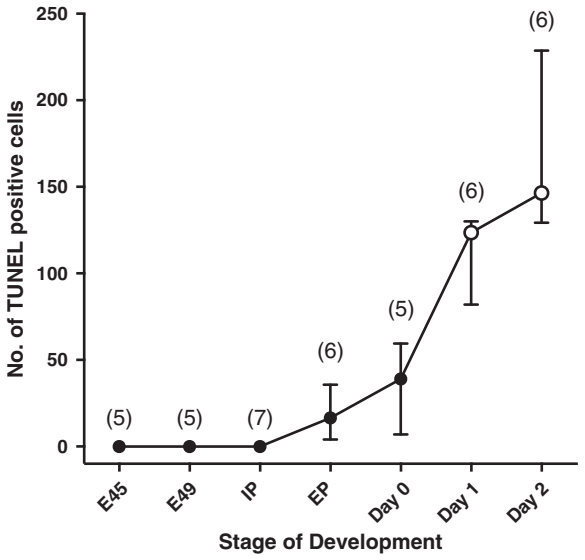

Fig. 4. Number of TUNEL-positive cells per field of observation as a function of hatching in the emu. Values are presented as the median and the 25th and 75th percentile. Sample sizes are provided in the parentheses. Open symbols represent a significant ($P < 0.05$) increase in number of TUNEL-positive cells per field of view compared with day 45 embryos.

increase in size during hatching. This change occurs earlier in the emu embryo than is observed in the chicken embryo, where similar changes in morphology do not occur until external pipping takes place (Belanger et al., 2008). This supports previous studies that state that mechanisms in the emu that regulate DA closure must mature earlier than those in the chicken (Crossley et al., 2003; Dzialowski and Greyner, 2007).

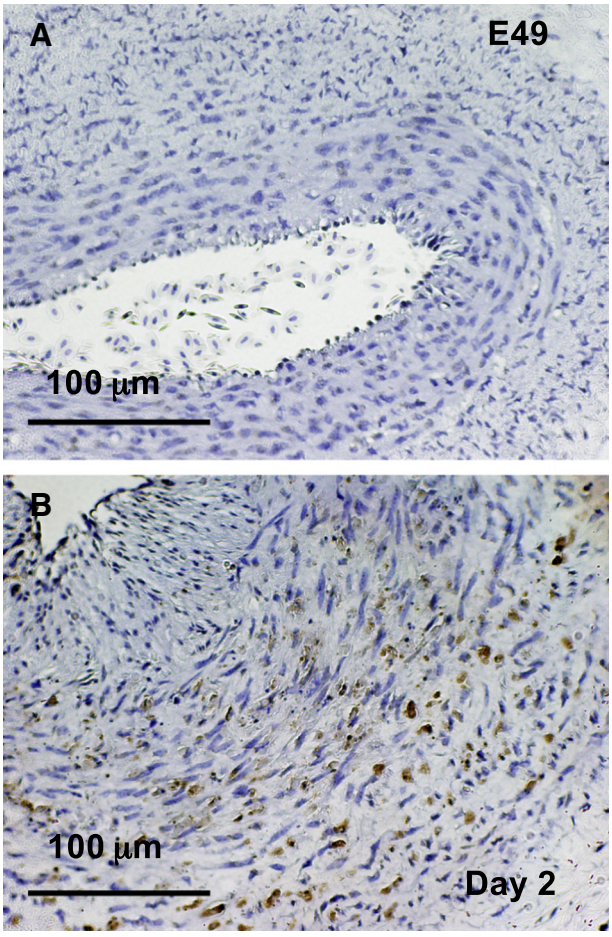

Fig. 5. Histological evidence for apoptosis in the DA during hatching. Representative histological sections of the DA stained for TUNEL-positive cells in A) a day 49 embryo and B) a day 2 hatchling. The nuclei stained brown in the day 2 hatchling are TUNEL-positive.

Smooth muscle cell migration coincides with the breakdown of the internal elastic lamina during IP. Comparative observations between smooth muscle cells and Van Gieson staining show that as the incidence of smooth muscle cells increase in the neointimal zone, the internal elastic lamina shows signs of disruption. Other studies of the DA in mammals and chickens have also noted the correlation between the introduction of smooth muscle cells into the neointimal zone and the breakdown of the internal elastic lamina (Slomp et al., 1997; Belanger et al., 2008). The fragmentation of elastin in the blood vessels of mice can induce the obstruction of a vessel through initiation of smooth muscle cell proliferation in the neointimal zone (Li et al., 1998). While molecules such as oxygen, epinephrine, and ATP have been linked to the regulation of DA closure, the disruption of the internal elastic lamina appears to ensure both the formation of intimal cushions and full DA occlusion (Li et al., 1998; Levin et al., 2005; Belanger et al., 2008). This might be especially true in bird and mammal species with larger DA lumens.

4.3. Apoptosis in the ductus arteriosus

The second stage of DA closure in mammals involves anatomical remodeling involving apoptosis (Clyman et al., 1999; Tananari et al., 2000). The extent and timing of apoptosis in the avian ductus during hatching is unknown. In this present study, the prevalence of apoptosis as indicated by the number of TUNEL-positive cells increased exponentially during and after hatching. Apoptotic cells began to appear during EP when the embryo begins pulmonary respiration. This time course is similar to that of the fetal and neonatal swine and lamb (Tananari et al., 2000; Levin et al., 2005). Apoptotic cells first appeared during the first four hours after birth in neonatal lambs and increased significantly at 14 to 24 h after birth. This correlates with the changes observed in the emu ductus, with the initial TUNEL-positive cells appearing during EP when the vessel first begins to constrict. Apoptosis occurs in the entirety of the DA in rabbits (Imamura et al., 2000), contrary to human DA closure where only inner media cells displayed apoptosis (Slomp et al., 1997). The presence of apoptotic cells in the emu aligns with the findings in rabbits, as TUNEL-positive smooth muscle cells are visible across the entire area of the vessel and were not isolated to one section but found in both the tunica media and adventitia. Significant numbers of TUNEL-positive cells differing from the day E45 vessels were seen in day 1 hatchlings and the first observation of cell death in the DA was seen in the IP stage of hatching. There was an exponential increase in the number of TUNEL-positive cells located in the tunica media upon hatching. There was also an exponential increase in the number of TUNEL-positive cells in the neonatal lamb DA following birth (Kajino et al., 2002)

As the DA constricts, its tissues should become hypoxic due to the decrease in blood flow through the vessel. This localized extreme hypoxia occurring during DA constriction results in a dramatic decrease in ATP concentration. This further contributes to the amount of cell death occurring in the DA after contraction (Levin et al., 2005). These drops in ATP levels, however, could be directly attributable to the loss of oxygen in the DA, which would leave the aerobic respiration pathways without a final electron acceptor, effectively cutting off the production of ATP through oxidative phosphorylation. This distinction, therefore, could simply be two sides of the same coin, with oxygen loss being the proximal cause of apoptosis, and ATP depletion being the ultimate causation. Another factor contributing to apoptosis in the DA, which would lead to a loss of ATP, is the depletion of glucose in the DA smooth muscle cells (Levin et al., 2005). Anaerobic respiration through glycolysis is the favored method of energy production, due to hypoxic conditions present in the DA. Hypoglycemia has a significant effect on the increased presence of TUNEL-positive cells in the DA.

Both of these phenomena could possibly attribute to DA cell death in the emu as during hatching when apoptotic cells increase significantly in number correlates with the constriction of the vessel (Fig. 5B).

4.4. Conclusions

Like mammals, all birds rely on a patent ductus arteriosus for blood flow during fetal development. However, the transition from the fetal gas exchanger to the lungs is prolonged in the birds. In the emu ductus closure begins on day 49 during the IP stage of hatching; at this point, the internal elastic lamina detaches from the endothelium and intimal cushions begin to form in the neointimal zone. The intimal cushions are composed of smooth muscle cells that have possibly migrated from the tunica media through the fragmented internal elastic lamina, evident from Van Gieson staining. The intimal cushions increase in size to occlude the lumen over the next several days and an exponential increase in apoptosis facilitates the anatomical remodeling of the vessel. These morphological changes all play a key role in permanently closing the DA in emu, and further studies should test the hypothesis that ATP depletion due to a decrease in glucose has a regulatory effect on the amount of cell death in the vessel.

Certainly, the large size of ratite eggs and embryos makes them a tractable model for studying avian ductus arteriosus morphology and physiology. However, whether the morphological and hemodynamic changes documented in the emu – a primitive ratite bird – are representative of other birds is not clear and begs further examination.

Acknowledgments

This study was supported by National Science Foundation Grant IOS0417205 awarded to EMD and National Science Foundation Grant IOS1025823 to WB. Steve Warburton provided help with the measurement of blood flow patterns during development.

References

Arciniegas, E., Ponce, L., Hartt, Y., Graterol, A., Carlini, R.G., 2000. Intimal thickening involves transdifferentiation of embryonic endothelial cells. Anat. Rec. 258, 47–57.
Belanger, C., Copeland, J., Muirhead, D., Heinz, D., Dzialowski, E.M., 2008. Morphological changes in the chicken ductus arteriosi during closure at hatching. Anat. Rec. 291, 1007–1015.
Bergwerff, M., DeRuiter, M.C., Gittenberger-de Groot, A.C., 1999. Comparative anatomy and ontogeny ofductus arteriosus, a vascular outsider. Anat. Embryol. 200, 559–571.
Clyman, R., Chan, C.Y., Mauray, F., Chen, Y.Q., Cox, W., Seidner, S.R., Lord, E.M., Weiss, H., Waleh, N., Evans, S.M., Koch, C.J., 1999. Permanent anatomic closure of the ductus arteriosus in newborn baboons: the roles of postnatal constriction, hypoxia, and gestation. Pediatr. Res. 45, 19–29.
Coceani, F., Baragatti, B., 2012. Mechanisms for ductus arteriosus closure. Semin. Perinatol. 36, 92–97.
Cogolludo, A.L., Moral-Sanz, J., van der Sterren, S., Frazziano, G., van Cleef, A.N.H., Menendez, C., Zoer, B., Moreno, E., Roman, A., Perez-Vizcaino, F., Villamor, E., 2009. Maturation of O_2 sensing and signaling in the chicken ductus arateriosus. Am. J. Physiol. Lung C. 297, L619–L630.
Crossley, D.A., Bagatto, B.P., Dzialowski, E.M., Burggren, W.W., 2003. Maturation of cardiovascular control mechanisms in the embryonic emu (*Dromiceius novaehollandiae*). J. Exp. Biol. 206, 2703–2710.
Dzialowski, E.M., Greyner, H., 2007. Maturation of the contractile response of the emu ductus arteriosus. J. Comp. Physiol. B. 178, 401–412.
Dzialowski, E.M., Sirsat, T., van der Sterren, S., Villamor, E., 2011. Prenatal cardiovascular shunts in amniotic vertebrates. Respir. Physiol. Neurobiol. 178, 66–74.
Gavrieli, Y., Sherman, Y., Ben-Sasson, S.A., 1992. Identification of programmed cell death in situ via specific labeling of nuclear DNA fragmentation. J. Cell Biol. 119, 493–501.
Giuriato, L., Scatena, M., Chiavegato, A., Guidolin, D., Pauletto, P., Sartore, S., 1993. Rabbit ductus arteriosus during development: anatomical structure and smooth muscle cell composition. Anat. Rec. 235, 95–110.
Goldbarg, S., Quinn, T., Waleh, N., Roman, C., Liu, B.M., Mauray, F., Clyman, R.I., 2003. Effects of hypoxia, hypoglycemia, and muscle shortening on cell death in the sheep ductus arteriosus. Pediatr. Res. 54, 204–211.
Greyner, H., Dzialowski, E.M., 2008. Mechanisms mediating the oxygen-induced vasoreactivity of the ductus arteriosus in the chicken embryo. Am. J. Physiol. Reg. I. 295, R1647–R1659.
Hong, Z., Kutty, S., Toth, P.T., Marsboom, G., Hammel, J.M., Chamberlain, C., Ryan, J.J., Zhang, H.J., Sharp, W.W., Morrow, E., Trivedi, K., Weir, E.K., Archer, S.L., 2013. Role of dynamin-related protein 1 (Drp1)-mediated mitochondrial fission in oxygen sensing and constriction of the ductus arteriosus. Circ. Res. 112, 802–815.
Imamura, S., Nishikawa, T., Hiratsuka, E., Takao, A., Matsuoka, R., 2000. Behavior of smooth muscle cells during arterial ductal closure at birth. J. Histochem. Cytochem. 48, 35–44.
Kajino, H., Goldbarg, S., Roman, C., Liu, B.M., Mauray, F., Chen, Y.Q., Takahashi, Y., Koch, C.J., Clyman, R.I., 2002. Vasa vasorum hypoperfusion is responsible for medial hypoxia and anatomic remodeling in the newborn lamb ductus arteriosus. Pediatr. Res. 51, 228–235.
Keck, M., Resnik, E., Linden, B., Anderson, F., Sukovich, D.J., Herron, J., Cornfield, D.N., 2005. Oxygen increases ductus arteriosus smooth muscle cytosolic calcium via release of calcium from inositol triphosphate-sensitive stores. Am. J. Physiol. Lung C. 288, L917–L923.
Kim, E.K., Kim, D.H., Choi, C.W., Kim, H.S., Kim, B.I., Choi, J.H., Kim, J.E., Kim, W.H., 2009. Insufficient intimal thickening and scarcity of cell deaths may play a significant role in the pathogenesis of the persistently patent ductus arteriosus in the preterm infant. Early Hum. Dev. 85, 181–186.
Levin, M., Goldbarg, S., Lindqvist, A., Sward, K., Roman, C., Liu, B.M., Hultén, L.M., Borén, J., Clyman, R., 2005. ATP depletion and cell death in the neonatal lamb ductus arteriosus. Pediatr. Res. 57, 801–805.
Levin, M., McCurnin, D., Seidner, S., Yoder, B., Waleh, N., Goldbarg, S., Roman, C., Liu, B.M., Borén, J., Clyman, R., 2006. Postnatal constriction, ATP depletion, and cell death in the mature and immature ductus arteriosus. Am. J. Physiol. Reg. I. 290, R359–R364.
Li, D.Y., Brooke, B., Davis, E.C., Mecham, R.P., Sorensen, L.K., Boak, B.B., Eichwald, E., Keating, M.T., 1998. Elastin is an essential determinant of arterial morphogenesis. Nature 393, 276–280.
Prum, R.O., Berv, J.S., Dornburg, A., Field, J.D., Townsend, J.P., Lemmon, E.M., Lemmon, A.R., 2015. A comprehensive phylogeny of birds (*Aves*) using targeted next-generation DNA sequencing. Nature 526, 569–573.
Rabinovitch, M., 1996. Cell–extracellular matrix interactions in the ductus arteriosus and perinatal pulmonary circulation. Semin. Perinatol. 20, 531–541.
Rahn, H., Matalon, S., Sotherland, P.R., 1985. Circulatory changes and oxygen delivery in the chick embryo prior to hatching. In: Johansen, K., Burggren, W.W. (Eds.), Cardiovascular Shunts. Munksgaard, Copenhagen, pp. 199–211.
Reese, J., Anderson, J.D., Brown, N., Roman, C., Clyman, R., 2006. Inhibition of cyclooxygenase isoforms in late- but not midgestation decreases contractility of the ductus arteriosus and prevents postnatal closure in mice. Am. J. Physiol. Reg. I. 291, R1717–R1723.
Rouwet, E.V., Tintu, A.N., Schellings, M.W., van Bilsen, M., Lutgens, E., Hofstra, L., Slaaf, D.W., Ramsay, G., Le Noble, F.A., 2002. Hypoxia induces aortic hypertrophic growth, left ventricular dysfunction, and sympathetic hyperinnervation of peripheral arteries in the chick embryo. Circulation 105, 2791–2796.
Sbong, S., Dzialowski, E.M., 2007. Respiratory and cardiovascular responses to acute hypoxia and hyperoxia in internally pipped chicken embryos. Comp. Biochem. Physiol. A Mol. Integr. Physiol. 148, 761–768.
Slomp, J., van Munsteren, J.C., Poelmann, R.E., de Reeder, E.G., Bogers, A.J.J.C., Gittenberger-de Groot, A.C., 1992. Formation of intimal cushions in the ductus arteriosus as a model for vascular intimal thickening: an immunohistochemical study of changes in extracellular matrix components. Atherosclerosis 93, 25–39.
Slomp, J., Gittenberger-de Groot, A.C., Glukhova, M.A., van Munsteren, J.C., Kockx, M.M., Schwartz, S.M., Koteliansky, V.E., 1997. Differentiation, dedifferentiation, and apoptosis of smooth muscle cells during the development of the human ductus arteriosus. Arterioscler. Thromb. Vasc. Biol. 17, 1003–1009.
Tada, T., Kishimoto, H., 1990. Ultrastructural and histological studies on closure of the mouse ductus arteriosus. Acta Anat. 139, 326–334.
Tananari, Y., Maeno, Y., Takagishi, T., Sasaguri, Y., Morimatsu, M., Kato, M.D., 2000. Role of apoptosis in the closure of neonatal ductus arteriosus. Jpn. Circ. J. 64, 684–688.
Tennenbaum, J.E., Waleh, N.S., Mauray, F., Gold, L., Perkett, E.A., Clyman, R.I., 1996. Transforming growth factor-β protein and messenger RNA expression is increased in the closing ductus arteriosus. Pediatr. Res. 39, 427–434.
Thébaud, B., Michelakis, E.D., Wu, X.C., Moudgil, R., Kuzyk, M., Dyck, J.R.B., Harry, G., Hashimoto, K., Harmony, A., Rebeyka, I., Archer, S.L., 2004. Oxygen-sensitive Kv channel gene transfer confers oxygen responsiveness to preterm rabbit and remodeled human ductus arteriosus: implications for infants with patent ductus arteriosus. Circulation 110, 1372–1379.
Tristani-Firouzi, M., Reeve, H.L., Tolarova, S., Weir, E.K., Archer, S.L., 1996. Oxygen-induced constriction of rabbit ductus arteriosus occurs via inhibition of a 4-aminopyridine-, voltage-sensitive potassium channel. J. Clin. Invest. 98, 1959–1965.
van der Sterren, S., Kessels, L., Perez-Vizcaino, F., Cogolludo, A.L., Villamor, E., 2014. Prenatal exposure to hyperoxia modifies the thromboxane prostanoid receptor-mediated response to H_2O_2 in the ductus arteriosus of the chicken embryo. J. Physiol. Pharmacol. 65, 283–293.
Visschedijk, A.H.J., 1968. The air space and embryonic respiration. 1. The pattern of gaseous exchange in the fertile egg during the closing stages of incubation. Br. Poult. Sci. 9, 173–184.
Weir, E.K., Obreztchikova, M., Vargese, A., Cabrera, J.A., Peterson, D.A., Hong, Z., 2008. Mechanisms of oxygen sensing: a key to therapy of pulmonary hypertension and patent ductus arteriosus. Br. J. Pharmacol. 155, 300–307.
Yokoyama, U., 2015. Prostaglandin E-mediated molecular mechanisms driving remodeling of the ductus arteriosus. Pediatr. Int. 57, 820–827.
Yokoyama, U., Minamisawa, S., Ishikawa, Y., 2010. Regulation of vascular tone and remodeling of the ductus arteriosus. J. Smooth Muscle Res. 46, 77–87.